https://doi.org/10.2352/issn.2168-3204.2023.20.1.26

A lens characterization method for low-budget high-quality museum photography

Alessandra Marrocchesi; University of Amsterdam and Rijksmuseum; Amsterdam, The Netherlands
Robert G. Erdmann; University of Amsterdam and Rijksmuseum; Amsterdam, The Netherlands

Abstract

Image sharpness is strongly dependent on lens aperture and camera position at capture. As high-end equipment is out of the reach of many museums, these choices are often mostly based on visual evaluations of image sharpness, which—though still possibly resulting in good quality images—is highly subjective and can lead to inconsistency. In the context of a broader effort to provide low-cost solutions for consistent high-quality museum photography, we propose a methodology for the characterization of the performance of a lens in terms of sharpness that enables the selection of the appropriate lens aperture and camera position for the capture of a sharp image of an object without the need for expensive equipment.

Introduction

Technical photography represents a fundamental technique within cultural heritage, providing a powerful tool in support of object documentation, conservation, and art-historical research. To ensure the reliability of the information extracted from photographs, it is of crucial importance that these are of high quality. The internationally recognized Metamorfoze [1] and FADGI [2] imaging guidelines are very useful in this sense, as they provide technical criteria and tolerances for the assessment of image quality. Meeting these—or even stricter—tolerances and obtaining high quality digital images means in practice that several factors concerning image capture and processing must be carefully addressed. Among these are the choice of lens aperture at capture and the camera focusing process, on which image sharpness is strongly dependent. In a typical workflow for the capture of a two-dimensional (2D) object—such as a painting or a work on paper—an aperture is chosen such that the corresponding depth of field allows for an acceptably sharp image across the entire subject, with a preference for those apertures that provide the sharpest images. Where this cannot be achieved, focus stacking might be carried out. Often the aperture choice is based on approximate depth of field calculations, available lens data and careful visual assessments of image sharpness at the different available settings. As autofocus is often not reliable or even not possible in the case of non-motorized lenses, the focusing process is typically carried out by moving the lens focus ring or the camera to a position where the corresponding image is visually evaluated as acceptably sharp. Though this way of proceeding might still result in valuable good quality images, it is highly subjective and can lead to inconsistent data. Furthermore, choosing the appropriate aperture for the capture of an object might be challenging, especially in high-resolution photography of objects with significant deviations from flatness, such as pastose paintings or paintings with a non-flat support. High-end solutions that overcome at least some of these difficulties are available, though far from accessible to most museums and conservation institutes. We hereby aim to overcome these limitations by proposing a lens characterization methodology that enables the selection of the appropriate lens aperture and camera position for the capture of a sharp image of a subject without the need for expensive equipment. In this proposal a brief review of the process of formation of focused and defocused images is followed by a description of the proposed methodology and the presentation of the results obtained.

Formation of focused and defocused images

In geometrical optics, the light rays from an object point P at distance u from a thin lens of focal length f are focused at the point Q on the image plane, situated at distance v behind the lens; u, v and f are related by:

$$\frac{1}{u} + \frac{1}{v} = \frac{1}{f}$$

In this view, an object point at distance $u' \neq u$ from the lens (i.e., out of focus) is imaged as a disk—the *circle of confusion*—at the image plane. A more realistic simple model is one that accounts for diffraction effects: if we consider an ideal lens with a circular aperture, a point source is imaged as an Airy pattern. Following the approach taken in [3][4], by approximating the Airy pattern with a Gaussian profile, the formation of a focused or defocused image can be expressed as a convolution of the input scene with a 2D Gaussian with standard deviation given by (Gaussian beam):

$$\sigma(z) = \sigma_0 \sqrt{\left(1 + \frac{z^2}{Z_R^2}\right)} \qquad (1)$$

where σ_0 is the standard deviation of the Gaussian approximating the Airy pattern at the image plane, z is the axial distance (in either direction) from the image plane and Z_R is given by:

$$Z_R = \pi \frac{\sigma_0^2}{\lambda}$$

where λ is the wavelength of the incoming radiation.

Proposed approach

It arises from this theoretical analysis that the position at which a camera should be placed to capture a focused image of an object—assuming a fixed magnification, i.e. no focus ring movement—can be estimated by taking a stack of pictures at different relative distances between the camera and the object and computing a focus measure for each of these images: the optimum camera position is estimated as the position where the focus measure reaches its maximum. Based on these considerations, at a high level, our procedure involves the following steps. First, a sequence of captures of a calibration target is made in which the camera is translated along the optical axis (z), ranging from too far to too close to the target to be in focus at a desired sampling

resolution. Then, for each image in the stack a local sharpness metric—to which we subsequently refer interchangeably with the term focus metric—is computed and downsampled, resulting in a stack of sharpness-metric images. Subsequently, at each pixel location a peaked sharpness vs. camera z-position curve is extracted and fitted with an analytical form to estimate its peak value, peak location, and full width at half maximum (FWHM). The result is a map of peak sharpness, camera z-position at peak sharpness, and depth of field at each location across the field of view. Additionally, this enables the estimation of the camera tilt relative to the flat target. When repeated across different apertures and sampling resolutions, the procedure enables detailed characterization of the performance of a given lens in terms of sharpness as a function of these quantities. Furthermore, the proposed system has several anticipated uses, including automatic camera placement, automatic selection of optimum aperture and computation of shape from focus, providing a general-purpose tool for the design and realization of a photographic campaign.

Focus metric operator

The principle underlying this way of proceeding is known from auto-focusing and—with slight variations—shape from focus applications, for which different focus measure operators have been proposed over the years [5]. In our approach, the squared Frobenius norm of the Hessian tensor ($\|H\|_F^2$) is used as the focus metric. Given the Hessian matrix for a 2D image function $L(x, y)$:

$$H = \begin{matrix} L_{xx} & L_{xy} \\ L_{yx} & L_{yy} \end{matrix}$$

That is:

$$\|H\|_F^2 = L_{xx}^2 + 2L_{xy}^2 + L_{yy}^2 \qquad (2)$$

which is a measure of local curvature: it is the squared sum of the principal curvatures at a given point (and basically corresponds to Koenderink's definition of *curvedness* [6]). In the proposed approach the focus metric expressed by (2) is computed through the convolution of finite difference filters with each image in the stack. The resulting images are then pyramid downsampled a number of times, according to the desired focus metric window size. In practice, the number of downsampling steps is computed so that the aggregated focus metric spans several of the checkerboard squares in the calibration target in order to ensure robustness to its exact placement and orientation.

Analytical form for fitting of focus vs. position

Once a stack of focus measure images has been collected, by plotting the focus measure at each pixel as a function of the camera z-position, a characteristic peaked focus curve is obtained. Different approaches have been proposed for fitting focus curves, such as Gaussian and Cauchy functions [3][7]. To determine which model best describes the focus curves obtained with the proposed Hessian-based focus measure operator, we simulated the capture of a stack of images of a checkerboard target at closely spaced camera z-positions by Gaussian blurring a synthetic image of a target according to (1). The focus measure operator (2) was applied to each image in the stack and averaged over the entire image, resulting in a dense sequence of simulated focus metrics as a function of z. Several analytical forms for peaked functions were tested for their fit to this data. Figure 1 summarizes the results. The average sharpness across the field of view is plotted as a function of the simulated camera displacement from the optimum focus position and a Gauss, Cauchy, and Student's t-function with two degrees of freedom are fitted to the data.

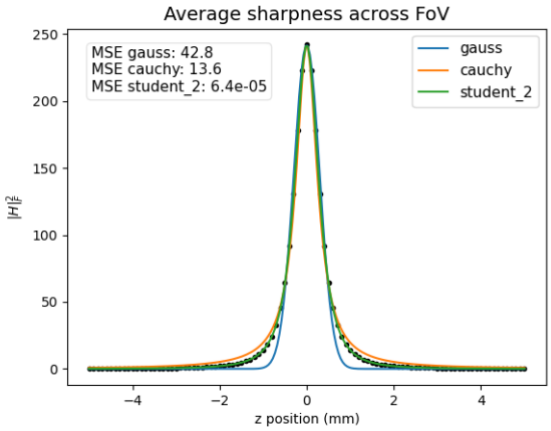

***Figure 1**. Average sharpness across the field of view as a function of camera displacement from the optimum focus position (simulated data). The curve is fitted with a Gauss, Cauchy, and Student's t-function with two degrees of freedom.*

Among the three functional forms tested, the best fit resulted from a vertically offset Student's t-function with two degrees of freedom:

$$f(z) = A\frac{B^3}{\left(\frac{1}{2}(z - z_0)^2 + B^2\right)^{\frac{3}{2}}} + C \qquad (3)$$

Where A is the amplitude, B is the half width at half maximum, z_0 represents the peak (or optimum focus) location and C is a constant offset. This model is therefore the one that we propose for fitting the focus curves from actual photographs.

Experimental procedure

For our image capture setup, we utilize a Canon EOS 5DS R camera (50.6 MP sensor with a pixel pitch of 4.14 µm) mounted on a computer-controlled motorized linear actuator providing motion along the optical (z) axis. As a calibration target, we utilize a checkerboard pattern printed on paper and attached to a rigid support. We carried out a performance characterization of two lenses: a Canon EF 50mm *f*/2.5 compact macro lens at 8.3 µm and 15 µm sampling resolution and a Canon TS-E 90mm *f*/2.8 at 15 µm sampling resolution. For each lens and chosen sampling resolution, a vertical stack of photographs of the calibration target was captured uniformly along the z axis for each available aperture. The square size of the checkerboard pattern was 1 mm for the lens characterization at 8.3 µm and 1.81 mm for the characterizations at 15 µm, to obtain the same square size (in pixels) in images at different sampling resolutions.

For each capture in a stack, the local focus metric (2) was calculated and pyramid downsampled 8 times, resulting in a sequence of focus metric versus camera-z for each position in the field of view. For each pixel in this reduced-resolution stack, this curve was fit with the analytical form (3) to obtain the camera z at peak focus, the peak focus value, and the full width at half maximum (FWHM) of the focus curve.

Results

In this section, the results achieved through our proposed methodology are summarized.

Here we detail the results for *f*/8 at 8.3 µm sampling resolution for the 50 mm lens. Figs. 2, 3, 4 and 5 respectively display: the estimated camera *z*-position for peak sharpness, the peak sharpness value, the FWHM of the fitted model and the mean squared error (MSE) of the fit across the field of view.

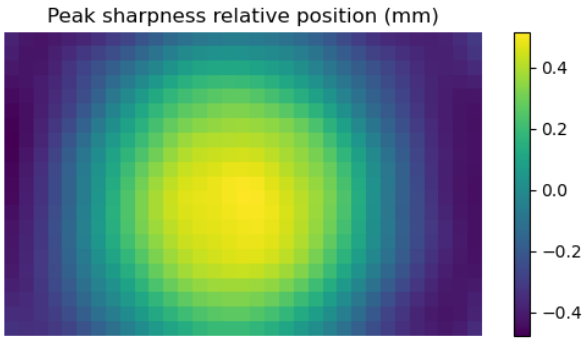

***Figure 2**. Estimated camera z-position for peak sharpness at f/8 and 8.3 µm sampling resolution (50 mm lens). The position is displayed as relative to the estimated optimum focus position.*

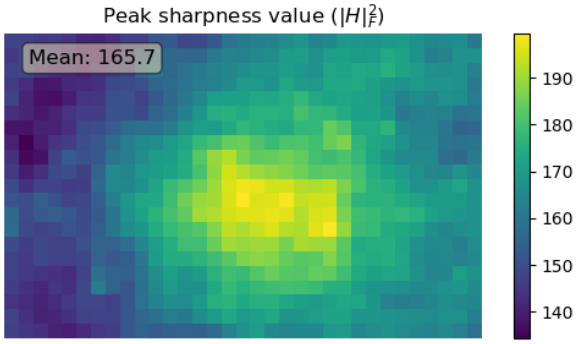

***Figure 3**. Estimated peak sharpness value at f/8 and 8.3 µm sampling resolution (50 mm lens).*

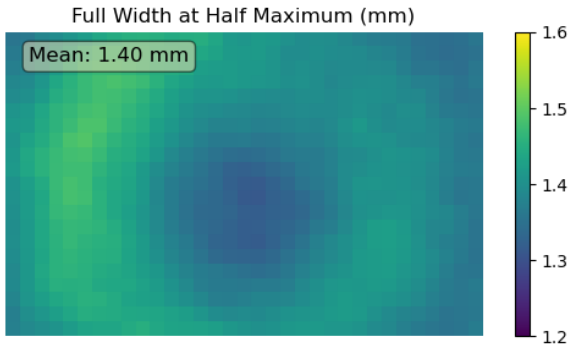

***Figure 4**. Estimated FWHM at f/8 and 8.3 µm sampling resolution (50 mm lens).*

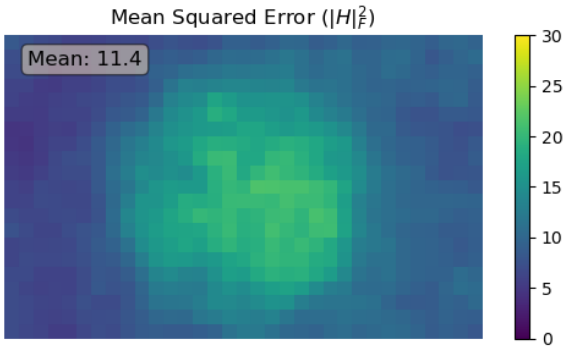

***Figure 5**. Estimated MSE of the fit at f/8 and 8.3 µm sampling resolution (50 mm lens).*

Fig. 6 shows a 3D plot of the peak sharpness position across the camera sensor (the same as plotted in Fig. 2) along with a fit with a planar surface and the estimated polar and azimuthal coordinates (θ, φ) of the corresponding surface normal. This provides an estimation of the tilt between the camera and the target and a characterization of field curvature.

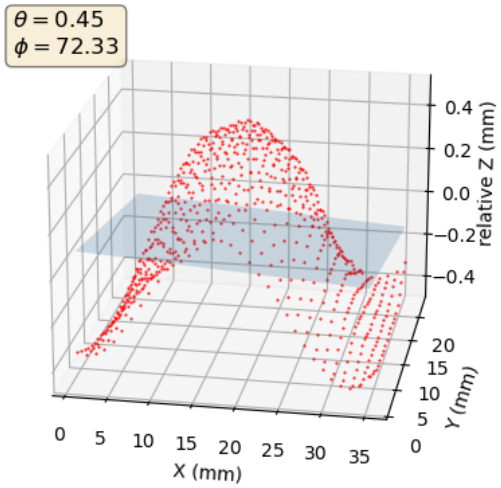

***Figure 6.** Estimated peak sharpness position across the camera sensor and fitted planar surface at f/8 and 8.3 µm sampling resolution (50 mm lens).*

Fig. 7 shows the focus measure average across the field of view as a function of the camera *z*-position along with a fit with (3). The peak position resulting from the fit is an estimate of the optimum focus position, i.e. the position where the camera should be moved to take the sharpest overall image of the subject.

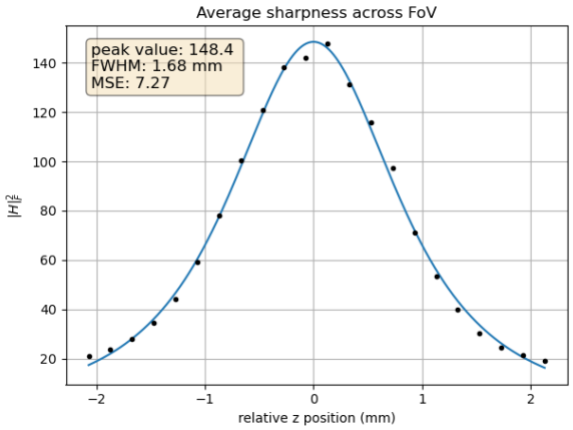

***Figure 7**. Average sharpness across the field of view as a function of the camera z-position at f/8 and 8.3 µm sampling resolution (50 mm lens). The position is displayed as relative to the peak position. The curve is fitted with (3).*

Aperture selection

Making use of the results of the fits of the average sharpness across the field of view from the different apertures it is possible to plot our sharpness measure as a function of camera *z*-position and aperture, as shown in Figure 8 with a contour plot.

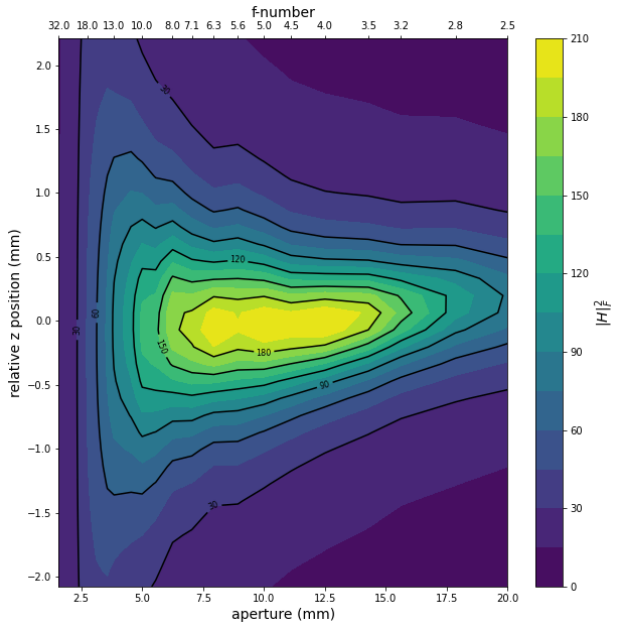

***Figure 8**. Modeled average sharpness across the field of view as a function of camera z-position and aperture (or f-number) at 8.3 µm sampling resolution for the 50 mm compact macro lens.*

The plot shows the effects of several phenomena. At the largest apertures, the effect of lens aberrations such as field curvature are relatively severe and the depth of field is narrow, resulting in relatively low peak sharpness values. For the smallest apertures, the depth of field is relatively large, but the effect of diffraction prevents the image from ever being sharp, even when the camera is ideally positioned. At intermediate apertures, the figure shows a "sweet spot" where the depth of field is relatively wide and the peak sharpness values are the highest achievable, since the effects of lens aberrations and of blurring due to diffraction are reduced.

The figure can also be used as a tool for aperture selection. For a given value of the focus metric corresponding to the user's conception of "acceptably sharp," it can be used as follows. For a given aperture, the intersection of a vertical line at that aperture with the contour will indicate the depth of field. An object displaying *z*-variation across the field of view, such as a pastose or curved painting, places constraints on the required depth of field to capture it sharply in a single shot. Thus, the plot allows the selection of the ideal aperture and working distance given the demands on average sharpness and the expected depth variation of the object to be photographed.

The results obtained at 15 µm sampling resolution for the 50 mm compact macro and 90 mm tilt-shift lens are respectively shown in Figures 9 and 10. As the two lenses were tested at the same sampling resolution of 15 µm, the two figures allow for a direct comparison of their performance in terms of sharpness at this sampling resolution.

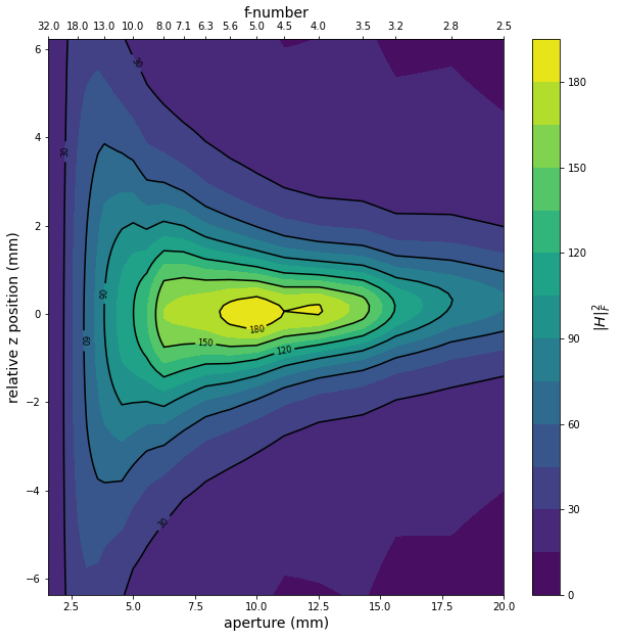

***Figure 9.** Modeled average sharpness across the field of view as a function of camera z-position and aperture (f-number) at 15 µm sampling resolution for the 50 mm compact macro lens.*

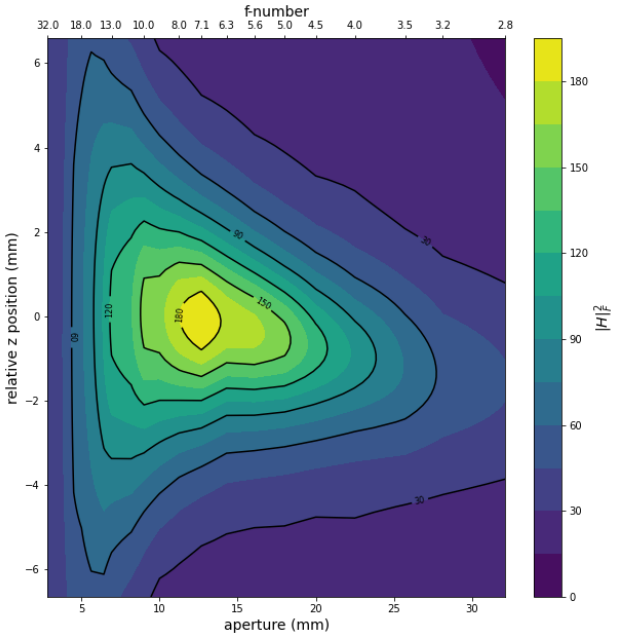

Figure 10. *Modeled average sharpness across the field of view as a function of camera z-position and aperture (f-number) at 15 µm sampling resolution for the 90 mm tilt-shift lens.*

Conclusions

In this paper, we presented a methodology that allows for a detailed characterization of a given lens in terms of sharpness based on the capture of a stack of images of a target with uniformly distributed features and the computation of a focus metric. A software tool has been developed such that, provided with the results of the lens characterization at different apertures, a required depth of field and a lower limit for image sharpness, it is able to compute which aperture choices can meet the requirements. This enables the automatic selection of the optimum aperture in the capture of an object. Furthermore, the image stack acquisition and processing procedure adopted for lens characterization can be applied for automatic camera placement at the best focus position in the imaging of an object. The proposed system can therefore be seen as a general-purpose tool for the design and realization of a photographic campaign.

The system proposed in this paper constitutes a component of a low-cost system for the technical photography of cultural heritage artifacts currently under development by the authors. The related software will be released as open source with the other components of the system.

References

[1] H. van Dormolen, Metamorfoze Preservation Imaging Guidelines. (2012).

[2] Federal Agencies Digital Guidelines Initiative, Technical Guidelines for Digitizing Cultural Heritage Materials. (2016).

[3] M. S. Muhammad and T.-S. Choi, 3D shape recovery by image focus using Lorentzian-Cauchy function, IEEE International Conference on Image Processing, pg. 4065–4068. (2010).

[4] M. Muhammad and T.-S. Choi, "Sampling for Shape from Focus in Optical Microscopy," IEEE Transactions on Pattern Analysis and Machine Intelligence, 34(3), 564–573 (2012).

[5] S. Pertuz, D. Puig and M. A. Garcia, "Analysis of focus measure operators for shape-from-focus," Pattern Recognition, 46(5), 1415–1432 (2013).

[6] J. J. Koenderink and A. J. van Doorn, "Surface shape and curvature scales," Image and Vision Computing, 10(8), 557–564 (1992).

[7] S. K. Nayar and Y. Nakagawa, "Shape from focus," IEEE Transactions on Pattern Analysis and Machine Intelligence, 16(8), 824–831 (1994).

Author Biography

Alessandra Marrocchesi is a PhD candidate at the University of Amsterdam within the EU-funded Marie Skłodowska-Curie Actions project Cultural Heritage Analysis for New Generations (CHANGE ITN) and a guest researcher at the Rijksmuseum. She graduated in 2019 with a Master's degree in Physics from the University of Pisa.

Robert G. Erdmann, Ph.D. is a Full Professor at the University of Amsterdam in the faculties of Science and of Humanities and is Senior Scientist at the Rijksmuseum. He was formerly associate professor of Materials Science and Engineering and of Applied Mathematics at the University of Arizona in Tucson, Arizona.